ACS APPLIED MATERIALS & INTERFACES

Research Article

www.acsami.org

Improve the Operational Stability of the Inverted Organic Solar Cells Using Bilayer Metal Oxide Structure

Jingjing Chang,[†] Zhenhua Lin,[‡] Changyun Jiang,[§] Jie Zhang,[§] Chunxiang Zhu,*[,‡] and Jishan Wu*[,†,§]

[†]Department of Chemistry, National University of Singapore, 3 Science Drive 3, Singapore 117543, Singapore

[‡]Department of Electrical and Computer Engineering, National University of Singapore, 10 Kent Ridge Crescent, Singapore 119260, Singapore

[§]Institute of Materials Research and Engineering, A*STAR, 3 Research Link, Singapore 117602, Singapore

Supporting Information

ABSTRACT: Operational stability is a big obstacle for the application of inverted organic solar cells (OSCs), however, less talked about in the research reports. Due to photoinduced degradation of the metal oxide interlayer, which can cause shunts generation and degeneration in ZnO interlayer, a significant degradation of open circuit voltage (V_{oc}) and fill factor (FF) has been observed by in situ periodic measurements of the device current density−voltage (J−V) curves with light illumination. By combining TiO_x and ZnO to form bilayer structures on ITO, the photovoltaic performance is improved and the photoinduced degradation is reduced. It was found that the device based on ZnO/TiO_x bilayer structure achieved better operational stability as compared to that with ZnO or TiO_x interlayer.

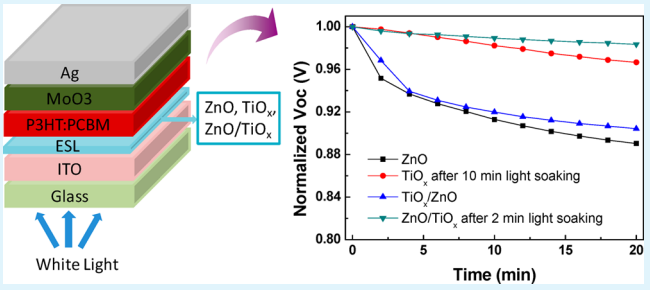

KEYWORDS: *inverted solar cell, metal oxide, ZnO, TiO_x, photoinduced degradation, bilayer structure*

INTRODUCTION

Inverted organic solar cells (OSCs) have attracted much attention due to the improved air stability compared with the conventional OSCs.[1−3] In the inverted structure, an *n*-type metal oxide film as the electron selective layer on an indium−tin-oxide (ITO) cathode and an air-stable and high-work-function metal such as silver or gold as the top anode are applied. Both the easily oxidized low-work-function metal and the easily corroded interface of ITO/poly(3,4-ethylenedioxythiophene):poly(styrenesulfonate) (PEDOT:PSS) used in conventional structure can be avoided, leading to high air stability. In inverted OSCs, one important issue to achieve high device performance is the electron selective layer (ESL). Several types of ESLs have been investigated and applied, such as metal oxides,[4−7] alkali salt,[8,9] and polyelectrolyte.[10−12] Among them, solution processed zinc oxide (ZnO) and titanium oxide (TiO_x) are good candidates to act as ESLs due to their high transmittance in visible range of spectra and low-temperature and roll-to-roll fabrication processability. Recently, solution processed ZnO and TiO_x have been largely used as the interlayer in solar cells through various methods, such as sol−gel chemistry, nanoparticle solution, and aqueous solution.

However, for a single metal oxide layer as the ESL, some key issues exist in the electrical properties of the oxide layer, limiting the device performance. For example, the low-temperature solution-processed ZnO layer has high surface defects (oxygen vacancy) that can act as a trap-assisted recombination center.[13,14] Oxygen desorption occurs in the ZnO layer under UV illumination, and the release of oxygen may induce a highly *n*-doped ZnO layer after a long time of UV illumination.[15] The high density traps caused by oxygen release in this highly *n*-doped ultrathin ZnO layer can significantly enhance the trap-assisted tunneling for both electrons and holes, thus reducing the capability of electron selectivity of the ZnO interlayer. This phenomenon causes ZnO based OSCs device degraded with UV illumination easily. While when use TiO_x as the ESL, the work function of the ITO/TiO_x surface has a little increase as compared to that of ITO-only surface, which causes a Schottky contact with the active layer and a large barrier blocking the electron transport to the cathode, resulting in an S-shaped J−V curve.[16−18] The work function can be decreased and the S-shape is eliminated after UV-illumination (light soaking) by surface band bending.[16] However, during this process, a harmful photo-oxidation in the organic active layer occurs, which also causes the device degradation.

Previously, bilayer metal oxides as the active layers in thin film transistors (TFTs) have been reported, and the results offered significant performance advantages by combining the

Received: July 18, 2014
Accepted: October 9, 2014
Published: October 9, 2014

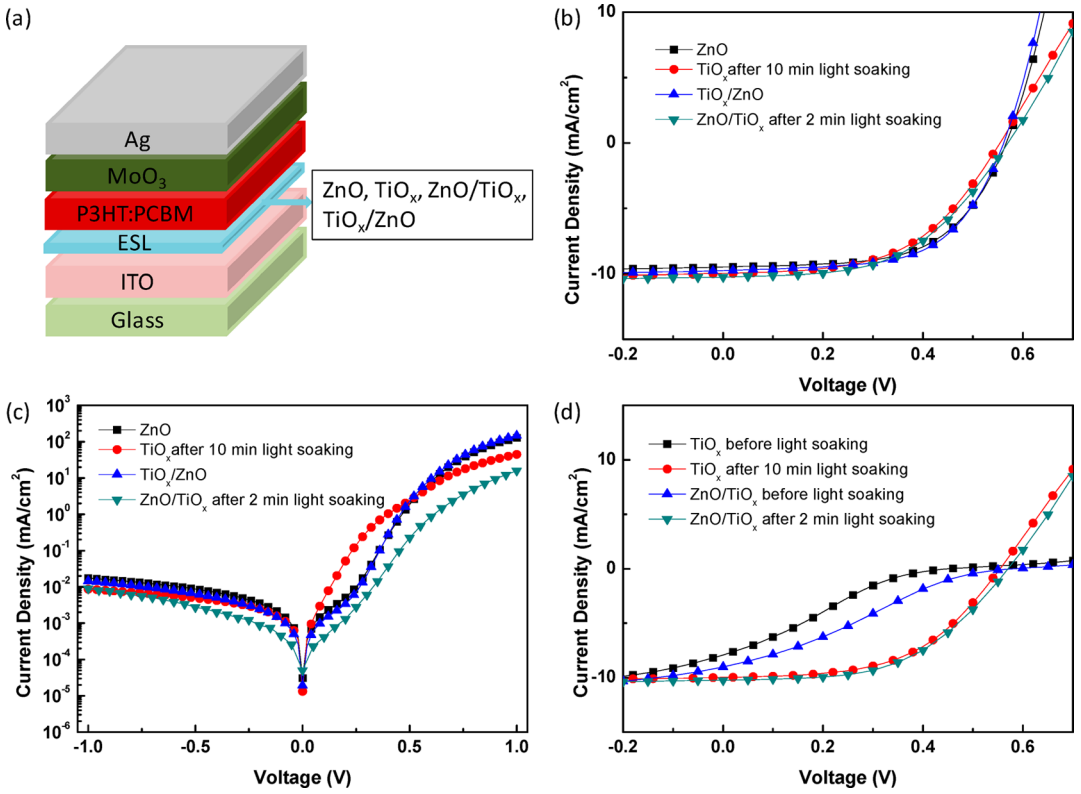

Figure 1. (a) Schematic of the device structure with metal oxide interlayer; (b,c) *J*–*V* characterisctics of inverted P3HT:$PC_{61}BM$ solar cells incorporating different ESLs under illumination and dark; (d) *J*–*V* characterisctics (under illumination) of inverted P3HT:$PC_{61}BM$ solar cells incorporating with TiO_x and ZnO/TiO_x ESLs before and after light soaking.

properties of the two semiconducting materials.[19,20] Compared to single layer devices, these bilayer devices effectively enhanced the photostability and suppressed normalized current noise spectral density. Therefore, the question is raised that whether it is possible to combine the highly conductive UV-unstable ZnO with low conductive UV-stable TiO_x to afford highly UV-stable and light-soaking-free devices. Recently, Riedl et al. reported the OSC devices based on atomic layer deposited (ALD) ZnO, TiO_x, Al-doped ZnO, and their combination bilayers.[16] It was found that the light soaking problem was due to the interface effect rather than the bulk electrical properties. Liu et al. reported the OSC devices using a solution-processed ZnO–TiO_x composite to enhance the photovoltaic performance of the solar cells.[21] However, the photostability of the devices based on solution-processed ZnO, TiO_x, and their combination bilayers has not been reported.

In this study, the photovoltaic performance and photo-induced degradation of inverted OSCs devices based on solution-processed TiO_x, ZnO, and bilayers of their combination as the ESL were studied and compared. It was found that using the ZnO/TiO_x bilayer structure as the ESL achieved not only an improved performance but also a better operational stability of the device as compared to that with single ZnO (or TiO_x) ESL.

EXPERIMENTAL SECTION

The cells were fabricated on ITO-coated glass substrates supplied by Xin Yan Technology LTD with a root-mean-square (RMS) surface roughness of 2–3 nm. The ITO substrates were cleaned by a routine solvent ultrasonic cleaning, sequentially with detergent, deionized water, acetone, and isopropyl alcohol (IPA) in an ultrasonic bath for 15 min each. For the ZnO layer preparation, first, ZnO nanopowder (Sigma-Aldrich) was directly dissolved in ammonia solution (0.1 M). After the ZnO particles were totally dissolved, the ZnO solution was spin-coated on top of ITO substrates at 3000 rpm for 30 s, and the formed ZnO films (~15 nm) were annealed at 120 °C for 10 min. For the TiO_x layer preparation, titanium isopropoxide (Sigma-Aldrich) was directly dissolved in IPA with a volume ratio of 1:200. The TiO_x solution was spin-coated on top of ITO substrates at 3000 rpm for 1 min, and the formed TiO_x films (~20 nm) were annealed at 120 °C for 10 min. For the bilayer structure, another TiO_x (or ZnO) layer was deposited on the ZnO (or TiO_x) layer (~30 nm) and also annealed at 120 °C for 10 min. Following that, an active layer was deposited on top of the metal oxide layer by spin-coating a solution of the poly(3-hexylthiophene) (P3HT, Rieke Metals) and phenyl-C61-butyric acid methylester (PCBM) (Nano-C) blend with a weight ratio of 1:1 in 1,2-dicholorobenzen (20 mg/mL) at 500 rpm for 130 s in a N_2 glovebox to produce a 180 nm thin film, and the active layers were preannealed at 140 °C for 10 min. Finally, a MoO_3 layer (6 nm) and a Ag layer (100 nm) were deposited on the active layers by using thermal evaporation. The device area is defined as 9 mm^2 by using a shadow mask. For each condition, four devices were prepared to give an average value. Figure 1a illustrates the schematic device structure of the inverted OSCs.

For the thin film transistor fabrication, a heavily doped *p*-type Si wafer (purchased from Silicon Quest International, Inc.) was used as substrate and gate electrode and 200 nm thermally grown SiO_2 was used as the dielectric layer. The substrates were cleaned with acetone, isopropyl alcohol (IPA), and deionized water, then treated with Ar plasma to facilitate metal oxide thin film formation. The ZnO thin film was formed as the above. Then, Al source/drain electrodes (100 nm thick) were deposited on top of the ZnO thin film with a shadow mask to finish the device. And selected devices were covered with TiO_x interlayer. The field-effect mobility of the fabricated transistor was extracted using the following equation in the saturation regime from the gate sweep: $I_D = W/(2L)C_i\mu(V_G-V_T)^2$, where I_D is the drain current in the saturated regime, μ is the field-effect mobility, C_i is the

Table 1. Device Photovoltaic Performance Parameters of Inverted P3HT:$PC_{61}BM$ Solar Cells Incorporating ZnO, TiO_x, TiO_x/ZnO and ZnO/TiO_x as the Electron Transport Layers

	interlayer	J_{sc} (mA/cm^2)	V_{oc} (V)	FF	η (%)
1	ZnO	9.50 ± 0.05	0.56 ± 0.004	0.58 ± 0.002	3.08 ± 0.05
2	TiO_x	9.97 ± 0.04	0.55 ± 0.004	0.53 ± 0.003	2.90 ± 0.04
3	TiO_x/ZnO	9.77 ± 0.03	0.57 ± 0.006	0.59 ± 0.005	3.28 ± 0.06
4	ZnO/TiO_x	10.25 ± 0.03	0.57 ± 0.002	0.54 ± 0.003	3.15 ± 0.03

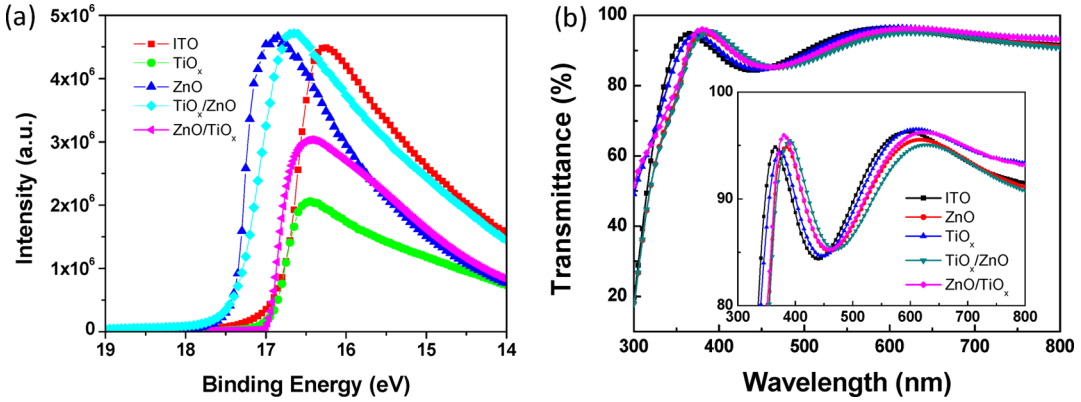

Figure 2. (a) UPS spectra of TiO_x, ZnO, TiO_x/ZnO, and ZnO/TiO_x deposited on top of ITO film and bare ITO film. (b) Transmittance of ZnO, TiO_x, TiO_x/ZnO, and ZnO/TiO_x films deposited on top of ITO film and bare ITO film.

capacitance per unit area of the gate dielectric layer (SiO_2, 200 nm, C_i = 17 nF cm^{-2}), V_G and V_T are gate voltage and threshold voltage, and W and L are channel width and length, respectively. The transistors were characterized with Keithley 4200 parameter analyzer in the N_2-filled glovebox and dark conditions.

The $J-V$ characteristics of the devices were measured using a Keithley 2400 parameter analyzer in the dark and under a simulated light (AM 1.5G) with intensity of 100 mW/cm^2 that was calibrated via a silicon reference cell. Incident photon-to-current efficiency (IPCE) measurements were performed under short circuit conditions with a lock-in amplifier (SR510, Stanford Research System) at a chopping frequency of 280 Hz during illumination with monochromatic light from a Xe arc lamp. The surface morphology and the roughness of the metal oxide films deposited on the ITO substrate were observed by tapping-mode atomic force microscopy (TM-AFM), which was performed on a Bruker ICON-PKG atomic force microscopy instrument. The film thickness was measured using a surface step profiler (KLA Tencor P15). The work-function of metal oxide layer was characterized by UPS experiments carried out on an Escalab 220i system in an ultrahigh vacuum, and He I (21.2 eV) as the excitation sources. The transmittance spectra of the metal oxide films deposited onto ITO/glass substrates were characterized using an UV-3600 Shimadzu UV−vis-NIR spectrophotometer.

RESULTS AND DISCUSSION

Figure 1b,c shows the $J-V$ characteristics under illumination (b) and dark (c) of four types of inverted devices with ESLs of ZnO, TiO_x, TiO_x/ZnO and ZnO/TiO_x, and the corresponding extracted device parameters are summarized in Table 1 and Figure S1 (Supporting Information). As shown in Figure 1b, the devices using the bilayer ESLs showed better performance than the devices with ZnO or TiO_x only ESL. Both V_{oc} and J_{sc} have been improved. The significant increase of J_{sc} for the device based on ZnO/TiO_x bilayer film compared with that based on ZnO only film was attributed to the reduced surface recombination by surface passivation.[18] And the slightly increased V_{oc} is due to the decreased work-function by charge transfer after light soaking. For the device based on the TiO_x/ZnO bilayer, the possible explanation for the improved device

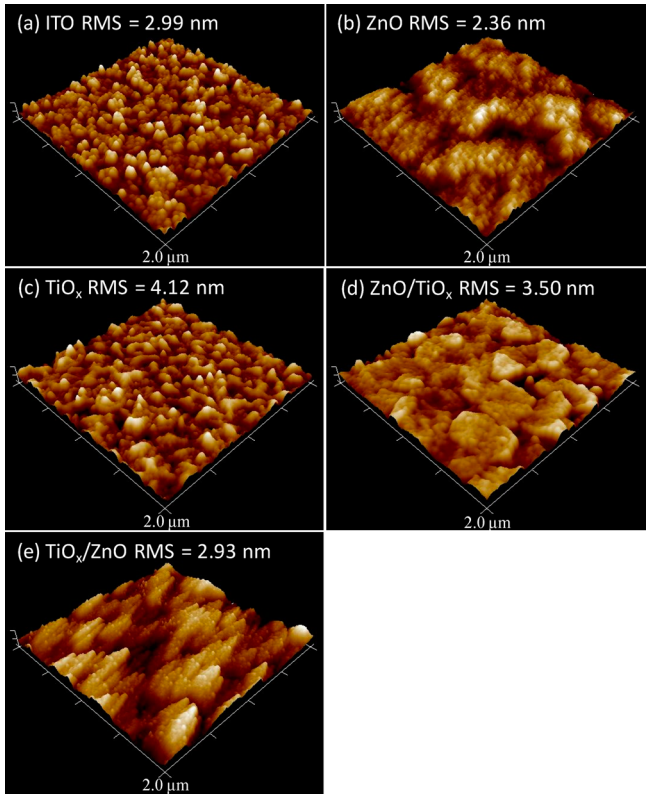

Figure 3. AFM images of (a) bare ITO film, and (b) ZnO, (c) TiO_x, (d) ZnO/TiO_x, and (e) TiO_x/ZnO films deposited on top of ITO films.

performance compared with that based on TiO_x or ZnO only film was due to the reduced series resistance and enhanced hole blocking capability. Figure 1d shows $J-V$ characteristics of inverted cells with TiO_x and ZnO/TiO_x ESLs before and after light soaking. The $J-V$ curves of both devices contained a kink

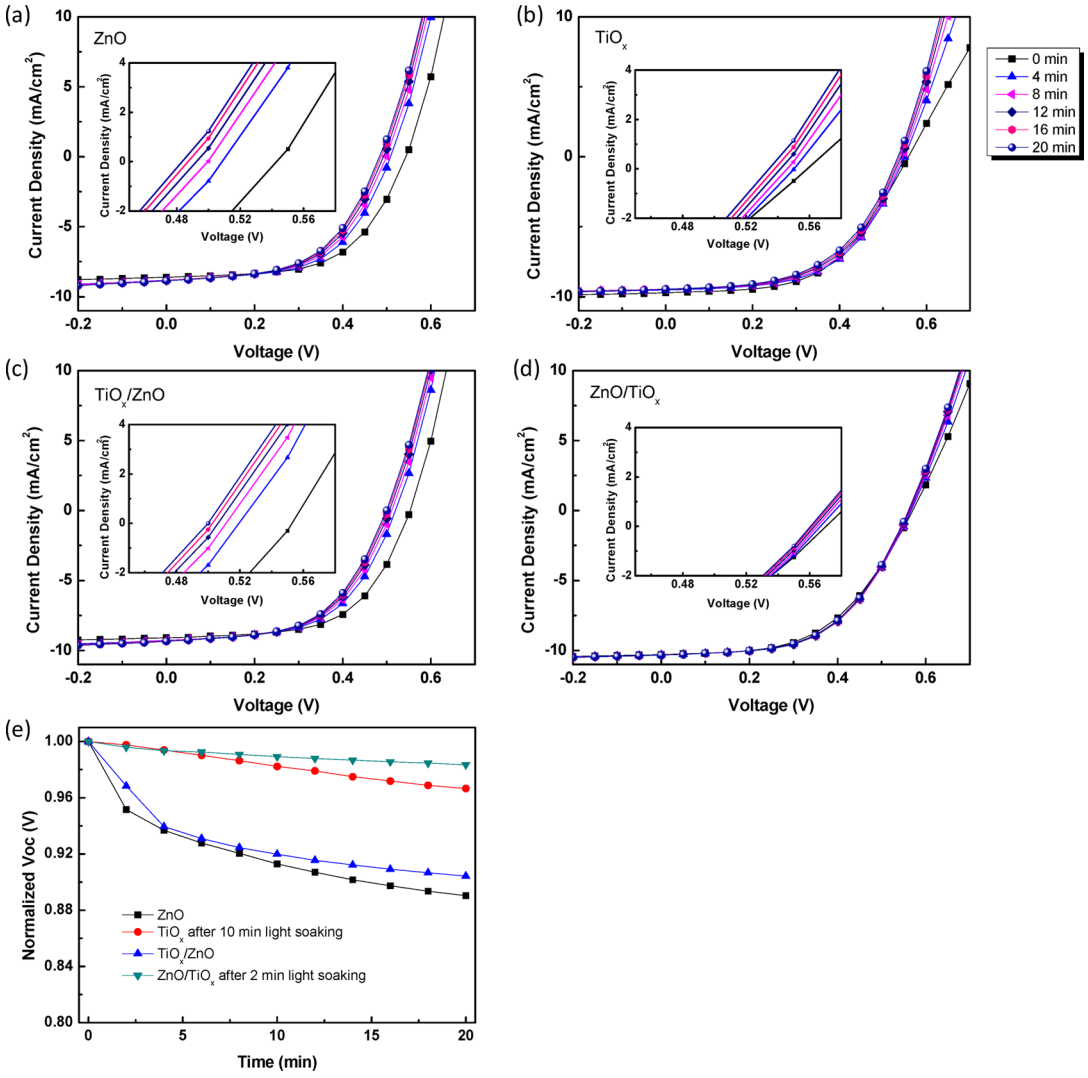

Figure 4. Periodic $J-V$ curve measurements for the devices based on (a) ZnO, (b) TiO_x, (c) TiO_x/ZnO, and (d) ZnO/TiO_x ESLs under illumination/operation for 20 min; (e) change of normalized V_{oc} with illumination time increased.

before light soaking. For the TiO_x only device, after light soaking for 10 min, a PCE of 2.9% could be achieved with a J_{sc} of 9.97 mA/cm^2, a V_{oc} of 0.55 V, and a fill factor of 0.53. The combination of ZnO and TiO_x layer (ZnO/TiO_x bilayer) not only reduced the light soaking time to 2 min, but also enhanced J_{sc} (10.25 mA/cm^2) and V_{oc} (0.57 V) simultaneously, which resulted in a higher PCE of 3.15% compared to that for TiO_x only devices (2.90%). The V_{oc} increased to 0.57 V; this could be explained by the charge transfer from highly conductive ZnO underlayer and charge states change of TiO_x. On the other hand, when a ZnO film was deposited on the TiO_x layer (TiO_x/ZnO bilayer), the S-shape in the $J-V$ curve could be eliminated (Figure 1b). The eliminated S-shape is due to the ohmic contact formed between ZnO and active layer, indicating that the S-shape behavior is only related with the metal oxide/active layer interfaces. This is confirmed by the UPS measurement (Figure 2a). The results show that the ITO/ZnO and ITO/TiO_x/ZnO films had similar surface work-functions, and had a decrease of about 0.7 eV compared with bare ITO surface. However, the ITO/TiO_x film had a similar surface work-function as the bare ITO surface.

The optical and morphological properties of each ELS deposited on the ITO/glass substrate have also been investigated. The transmittances of the ESL films are shown in Figure 2b. It can be seen that the TiO_x layer has better transmittance than the ZnO layer, and the transmittance of the ZnO and TiO_x single layer was less affected after deposited with another type of layer. The surface roughness of each electrode has also been characterized by AFM, as shown in Figure 3. The RMS values of surface roughness are 2.99, 2.36, 4.12, 3.50 and 2.93 nm for bare ITO, ITO/ZnO, ITO/TiO_x, ITO/ZnO/TiO_x, and ITO/TiO_x/ZnO, respectively. It was observed that the roughness decreases with ZnO layer deposition but increases with TiO_x layer deposition, which may be due to some aggregation of the TiO_x particles.

To investigate the device operational stability, the devices were kept under illumination and in situ measured periodically to observe the illumination/operation degradation effect on the device performance. Figure 4a–d shows the $J-V$ curves periodically measured for the devices based on different ESLs under illumination for 20 min, and Figure 4e shows the change of normalized V_{oc} with time. It can be seen that the performance of all the devices decreased with the illumination/operation time, especially the V_{oc} values. From Figure 4e, the V_{oc} of the devices with TiO_x/active-layer contacts decreased more slowly than those with ZnO/active-layer contacts. The

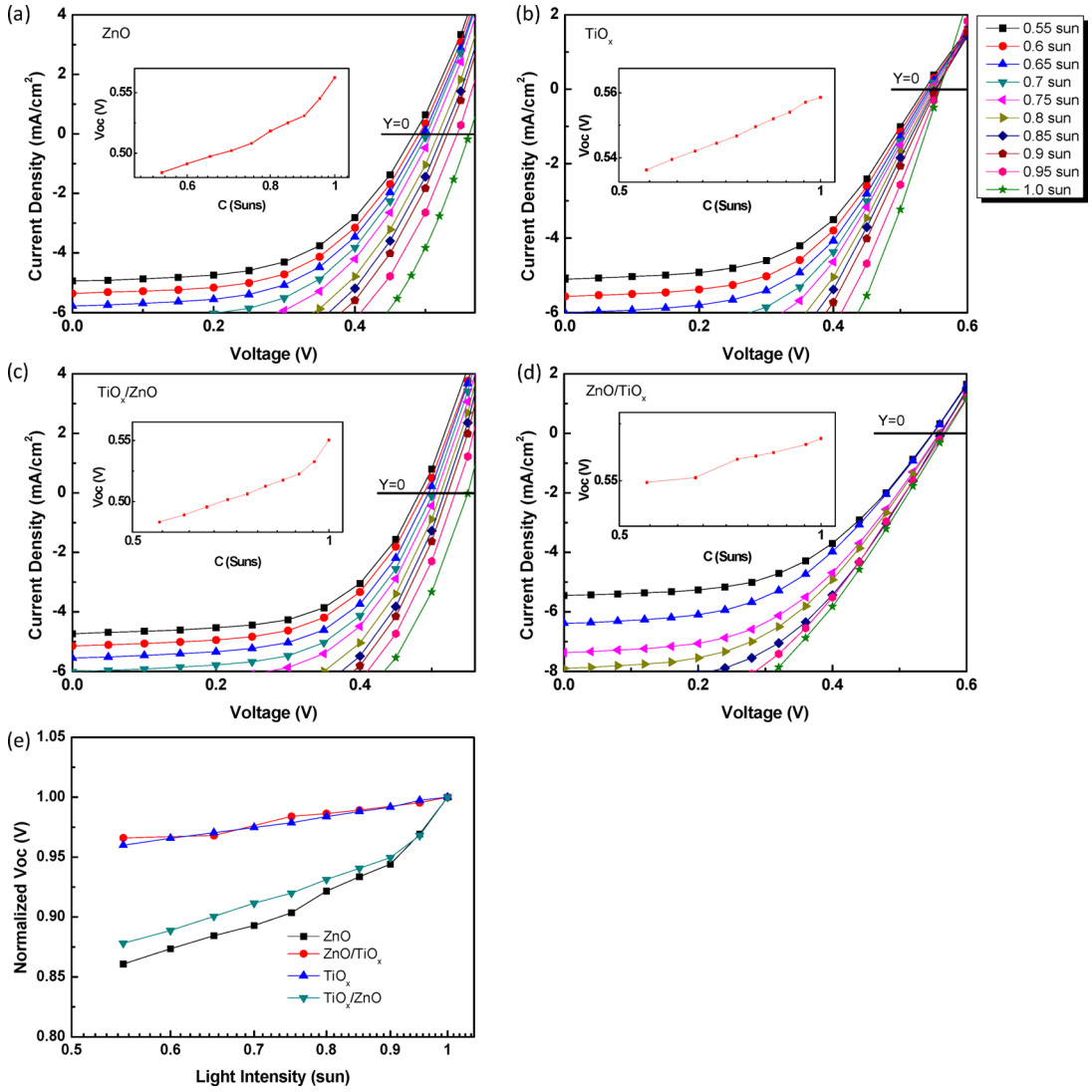

Figure 5. $J-V$ characteristics of the device performance with different light intensities for devices based on (a) ZnO, (b) TiO_x, (c) TiO_x/ZnO, and (d) ZnO/TiO_x ESLs; (e) light intensity dependence of normalized V_{oc}.

V_{oc} of the device based on ZnO-only ESL had a most rapid and significant decrease among those devices, with only 89% of the original V_{oc} value remained after 20 min of illumination. However, the device based on ZnO/TiO_x ESL shows the most stable performance, with 98.3% of the original V_{oc} value retained after 20 min of illumination.

The $J-V$ characteristics of the device performance with different light intensities have been measured for those devices, as shown in Figure 5a–d, and the V_{oc} as a function of the light intensity is presented in the inset graphs. Figure 5e shows the light intensity dependence of normalized V_{oc} of all those devices. Theoretically, the V_{oc} is expressed by $V_{oc} \approx (nkT/q) \ln(I_{sc}/I_0) = (nkT/q) \ln(C)$ + constant, where n, k, T, q, I_0 and C are the ideality factor, the Boltzmann constant, the temperature, the electron charge, the photocurrent and the concentration of the sunlight delivered to the cell, respectively.[22] From this equation, the value of n can be estimated by the slope of $(nkT/q) \ln(C)$. From Figure 5e, it can be observed that $n_{ZnO} \geq n_{TiOx/ZnO} > n_{TiOx} \geq n_{ZnO/TiOx}$. The ideality factor is a good tool to analyze the transport and recombination process. A higher ideality factor extracted from V_{oc} means a larger shunting effect caused by higher trap-assisted recombination.[23]

The possible physical mechanism of the shunting effect for the device based on the ZnO film has already been reported.[15] The oxygen desorption in the ZnO layer under illumination induces a narrow bandwidth, which reduces the ZnO capability to act as the ESL. However, when an additional TiO_x film was added, the TiO_x layer was in contact with active layer and played the hole-blocking role. When TiO_x layer was deposited on top of the ZnO film, the charge transfer from conductive ZnO to the TiO_x surface could occur and cause band bending on the TiO_x surface, leading to a lower TiO_x work-function. This could be the possible explanation for the reduced light soaking time of the device based on ZnO/TiO_x film compared with that based on the bare TiO_x film.

To prove the charge transfer between the ZnO and TiO_x, the thin film transistors based on the ZnO thin film were fabricated. As shown in Figure 6, the bare ZnO device showed a dark saturation current of around 80 μA. Under white light illuminance for 10 min, the maximium drain current increased up to about 2 mA, which is about 25× higher than the dark saturation current, and the charge carrier mobility increased from 0.32 to 0.88 $cm^2\ V^{-1}\ s^{-1}$. This could be explained by the light induced free electron carrier increase due to the oxygen

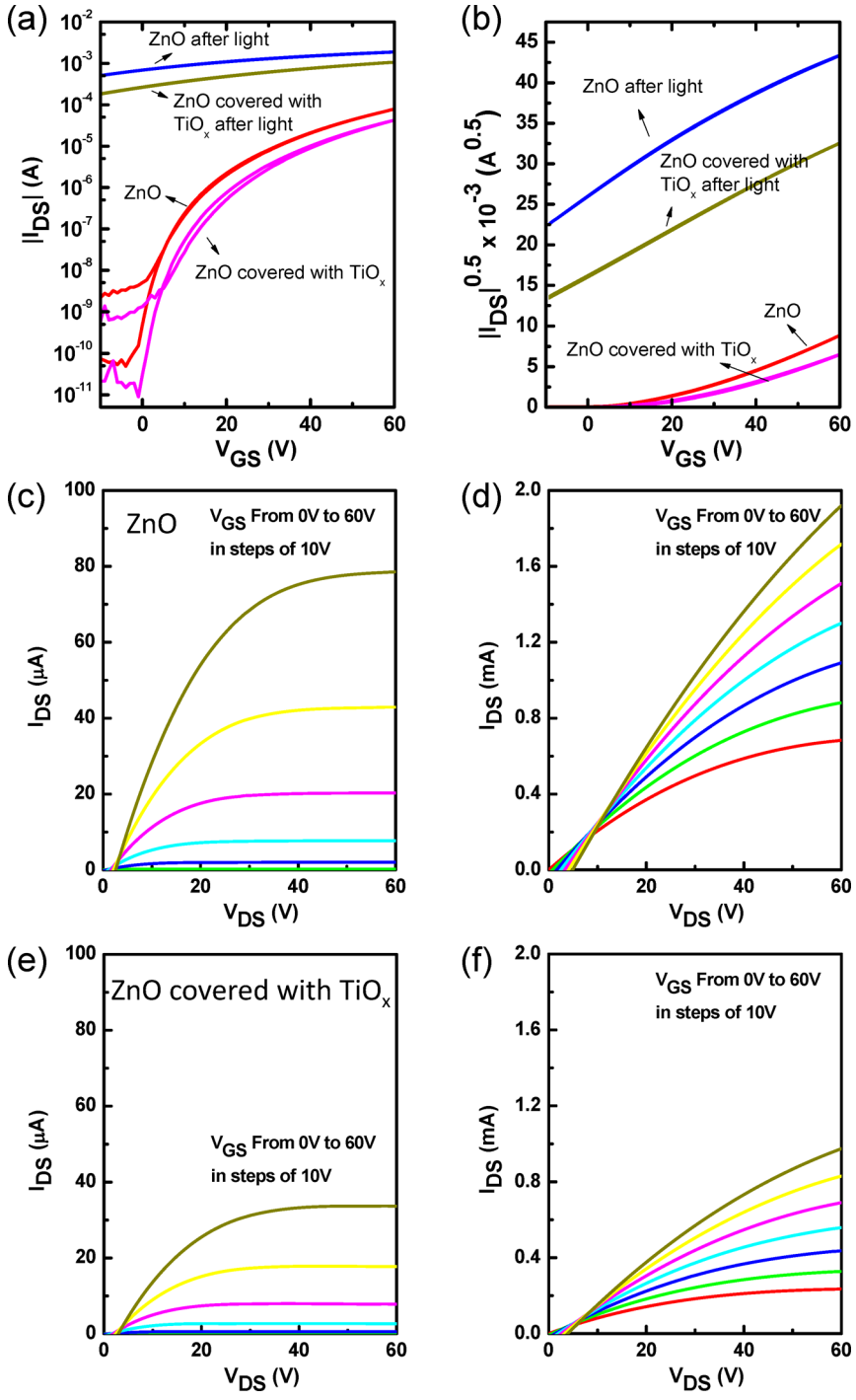

Figure 6. Transfer (a,b) and output (c–f) curves of the ZnO devices with different treatments tested in dark condition. (c) Bare ZnO device. (d) ZnO device was treated with 10 min light illumination. (e) ZnO device was covered with TiO_x layer. (f) ZnO device covered with TiO_x layer was treated with 10 min of light illumination.

vacancy state change.[24,25] After the device was coated with the TiO_x layer, the drain current decreased compared to the bare ZnO based device for both of the dark current and photocurrent, indicating that a charge transfer occurs from ZnO (electron donor) to TiO_x (electron acceptor). This is consistent with the literature reported that when ZnO interacts with the gas molecules or the organic layer, the charge transfer could occur.[26−28] For TiO_x, when it is in contact with ZnO, it could accept electrons, which causes electrons to accumulate at the surface, and the bands are bent such that the surface electron density increases.

CONCLUSIONS

In summary, the performance and photoillumination/operation stability of the inverted organic solar cell devices with different metal oxide ESLs were studied. Due to the shunts generation and degeneration in ZnO layer, a significant degradation of V_{oc} has been observed for the device based on the ZnO ESL. Moderate degradation was also observed from the device based

on the TiO_x layer, which required light-soaking to remove the Schottky barrier at the TiO_x/P3HT interface. By combining ZnO and TiO_x to form bilayer ESLs on ITO (either TiO_x/ZnO or ZnO/TiO_x), the devices showed improved photovoltaic performances, and the device based on ZnO/TiO_x achieved the highest photocurrent and the best stability under photo-illumination.

■ ASSOCIATED CONTENT

Supporting Information

Device-to-device variations of PCEs of the solar cells with different interlayers. This material is available free of charge via the Internet at http://pubs.acs.org.

■ AUTHOR INFORMATION

Corresponding Authors

*J. Wu. Fax: +65 6779 1691. Tel: +65 6516 2677. E-mail: chmwuj@nus.edu.sg.

*C. Zhu. E-mail: elezhucx@nus.edu.sg.

Notes

The authors declare no competing financial interest.

■ ACKNOWLEDGMENTS

This work was financially supported by MOE Tier 2 grant (MOE2011-T2-2-130), IMRE Core Funding (IMRE/13-1C0205), A*STAR SERC TSRP grant (Grant #102 170 0137), and A*STAR IMRE/10-1P0508.

■ REFERENCES

(1) Jørgensen, M.; Norrman, K.; Gevorgyan, S. A.; Tromholt, T.; Andreasen, B.; Krebs, F. C. Stability of Polymer Solar Cells. *Adv. Mater.* **2012**, *24*, 580−612.

(2) Yip, H.-L.; Jen, A. K.-Y. Recent Advances in Solution-Processed Interfacial Materials for Efficient and Stable Polymer Solar Cells. *Energy Environ. Sci.* **2012**, *5*, 5994−6011.

(3) Chen, L. M.; Hong, Z.; Li, G.; Yang, Y. Recent Progress in Polymer Solar Cells: Manipulation of Polymer:Fullerene Morphology and The Formation of Efficient Inverted Polymer Solar Cells. *Adv. Mater.* **2009**, *21*, 1434−1449.

(4) Sun, Y.; Seo, J. H.; Takacs, C. J.; Seifter, J.; Heeger, A. J. Inverted Polymer Solar Cells Integrated with a Low-Temperature-Annealed Sol-Gel-Derived ZnO Film as an Electron Transport Layer. *Adv. Mater.* **2011**, *23*, 1679−1683.

(5) Liang, Z.; Zhang, Q.; Wiranwetchayan, O.; Xi, J.; Yang, Z.; Park, K.; Li, C.; Cao, G. Effects of the Morphology of a ZnO Buffer Layer on the Photovoltaic Performance of Inverted Polymer Solar Cells. *Adv. Funct. Mater.* **2012**, *22*, 2194−2201.

(6) Chang, J.; Lin, Z.; Zhu, C.; Chi, C.; Zhang, J.; Wu, J. Solution-Processed LiF-Doped ZnO Films for High Performance Low Temperature Field Effect Transistors and Inverted Solar Cells. *ACS Appl. Mater. Interfaces* **2013**, *5*, 6687−6693.

(7) Chang, J.; Kam, Z. M.; Lin, Z.; Zhu, C.; Zhang, J.; Wu, J. TiO_x/Al Bilayer as Cathode Buffer Layer for Inverted Organic Solar Cell. *Appl. Phys. Lett.* **2013**, *103*, 173303.

(8) Li, G.; Chu, C.-W.; Shrotriya, V.; Huang, J.; Yang, Y. Efficient Inverted Polymer Solar Cells. *Appl. Phys. Lett.* **2006**, *88*, 253503.

(9) Liao, H.-H.; Chen, L.-M.; Xu, Z.; Li, G.; Yang, Y. Highly Efficient Inverted Polymer Solar Cell by Low Temperature Annealing of Cs_2CO_3 Interlayer. *Appl. Phys. Lett.* **2008**, *92*, 173303.

(10) He, Z.; Zhong, C.; Su, S.; Xu, M.; Wu, H.; Cao, Y. Enhanced Power-Conversion Efficiency in Polymer Solar Cells using an Inverted Device Structure. *Nat. Photonics* **2012**, *6*, 591−595.

(11) Kang, H.; Hong, S.; Lee, J.; Lee, K. Electrostatically Self-Assembled Nonconjugated Polyelectrolytes as an Ideal Interfacial Layer for Inverted Polymer Solar Cells. *Adv. Mater.* **2012**, *24*, 3005−3009.

(12) Lin, Z.; Chang, J.; Zhang, J.; Jiang, C.; Wu, J.; Zhu, C. A Work-Function Tunable Polyelectrolyte Complex (PEI:PSS) as a Cathode Interfacial Layer for Inverted Organic Solar Cells. *J. Mater. Chem. A* **2014**, *2*, 7788−7794.

(13) Hsieh, C.-H.; Cheng, Y.-J.; Li, P.-J.; Chen, C.-H.; Dubosc, M.; Liang, R.-M.; Hsu, C.-S. Highly Efficient and Stable Inverted Polymer Solar Cells Integrated with a Cross-Linked Fullerene Material as an Interlayer. *J. Am. Chem. Soc.* **2010**, *132*, 4887−4893.

(14) Shao, S.; Zheng, K.; Pullerits, T.; Zhang, F. Enhanced Performance of Inverted Polymer Solar Cells by Using Poly(ethylene oxide)-Modified ZnO as an Electron Transport Layer. *ACS Appl. Mater. Interfaces* **2013**, *5*, 380−385.

(15) Manor, A.; Katz, E. A.; Tromholt, T.; Krebs, F. C. Electrical and Photo-Induced Degradation of ZnO Layers in Organic Photovoltaics. *Adv. Energy Mater.* **2011**, *1*, 836−843.

(16) Trost, S.; Zilberberg, K.; Behrendt, A.; Polywka, A.; Görrn, P.; Reckers, P.; Maibach, J.; Mayer, T.; Riedl, T. Overcoming the "Light-Soaking" Issue in Inverted Organic Solar Cells by the Use of Al:ZnO Electron Extraction Layers. *Adv. Energy Mater.* **2013**, *3*, 1437−1444.

(17) Lin, Z.; Jiang, C.; Zhu, C.; Zhang, J. Development of Inverted Organic Solar Cells with TiO_2 Interface Layer by Using Low-Temperature Atomic Layer Deposition. *ACS Appl. Mater. Interfaces* **2013**, *5*, 713−718.

(18) Schmidt, H.; Zilberberg, K.; Schmale, S.; Flügge, H.; Riedl, T.; Kowalsky, W. Transient Characteristics of Inverted Polymer Solar Cells Using Titaniumoxide Interlayers. *Appl. Phys. Lett.* **2010**, *96*, 243305.

(19) Kim, H.-S.; Park, J. S.; Jeong, H. K.; Son, K. S.; Kim, T. S.; Seon, J.-B.; Lee, E.; Chung, J. G.; Kim, D. H.; Ryu, M.; Lee, S. Y. Density of States-based Design of Metal Oxide Thin-Film Transistors for High Mobility and Superior Photostability. *ACS Appl. Mater. Interfaces* **2012**, *4*, 5416−5421.

(20) Yu, X.; Zhou, N.; Smith, J.; Lin, H.; Stallings, K.; Yu, J.; Marks, T. J.; Facchetti, A. Synergistic Approach to High-Performance Oxide Thin Film Transistors Using a Bilayer Channel Architecture. *ACS Appl. Mater. Interfaces* **2013**, *5*, 7983.

(21) Liu, J.; Shao, S.; Meng, B.; Fang, G.; Xie, Z.; Wang, L.; Li, X. Enhancement of Inverted Polymer Solar Cells with Solution-Processed ZnO-TiO_x Composite as Cathode Buffer Layer. *Appl. Phys. Lett.* **2012**, *100*, 213906.

(22) Tromholt, T.; Katz, E. A.; Hirsch, B.; Vossierand, A.; Krebs, F. C. Effects of Concentrated Sunlight on Organic Photovoltaics. *Appl. Phys. Lett.* **2010**, *96*, 073501.

(23) Wetzelaer, G. A. H.; Kuik, M.; Lenes, M.; Blom, P. W. M. Origin of The Dark-Current Ideality Factor in Polymer:Fullerene Bulk Heterojunction Solar Cells. *Appl. Phys. Lett.* **2011**, *99*, 153506.

(24) Görrn, P.; Lehnhardt, M.; Riedl, T.; Kowalsky, W. The Influence of Visible Light on Transparent Zinc Tin Oxide Thin Film Transistors. *Appl. Phys. Lett.* **2007**, *91*, 193504.

(25) Chowdhury, M. D. H.; Migliorato, P.; Jang, J. Light Induced Instabilities in Amorphous Indium−Gallium−Zinc−Oxide Thin-Film Transistors. *Appl. Phys. Lett.* **2010**, *97*, 173506.

(26) Park, J.-S.; Jeong, J. K.; Chung, H.-J.; Mo, Y.-G.; Kim, H. D. Electronic Transport Properties of Amorphous Indium-Gallium-Zinc Oxide Semiconductor Upon Exposure to Water. *Appl. Phys. Lett.* **2008**, *92*, 072104.

(27) Spalenka, J. W.; Gopalan, P.; Katz, H. E.; Evans, P. G. Electron Mobility Enhancement in ZnO Thin Films Via Surface Modification by Carboxylic Acids. *Appl. Phys. Lett.* **2013**, *102*, 041602.

(28) Allen, C. G.; Baker, D. J.; Albin, J. M.; Oertli, H. E.; Gillaspie, D. T.; Olson, D. C.; Furtak, T. E.; Collins, R. T. Surface Modification of ZnO Using Triethoxysilane-based Molecules. *Langmuir* **2008**, *24*, 13393−13398.